Forest Analysis by Single-Pass Millimeterwave SAR Tomography

Michael Schmitt[1], Xiao Xiang Zhu[1,2]
[1]Signal Processing in Earth Observation, Technical University of Munich (TUM), Munich, Germany
[2]Remote Sensing Technology Institute, German Aerospace Center (DLR), Oberpfaffenhofen, Germany

Abstract

Recent investigations show that millimeterwave SAR tomography provides an interesting means for the analysis of forested areas, especially if single-pass systems are employed. Providing very high resolutions in the decimeter domain and highly coherent data also for slightly windy conditions, even individual trees can be considered. Besides, it has been shown that a certain amount of canopy penetration is possible in spite of the short wavelength.

1 Introduction

Since the principle of SAR tomography (TomoSAR) was practically demonstrated for the first time by Reigber & Moreira [1], the volumetric analysis of forested areas has been a research topic of steady interest. However, most of the literature only investigated the use of long-wavelength radar, such as L-band or P-band (e.g. [2-4]). Only few experiments have investigated the potential of shorter wavelength SAR using X-band sensors instead [5].

Going in the opposite direction, the use of millimeterwave SAR has been suggested for the analysis of forested areas some years ago for the first time, which already led to successful investigations aiming at the generation of 3D point clouds using a TomoSAR model for discrete scattering profiles [6]. The resulting point clouds have then been used for the reconstruction of individual tree models including core parameters such as tree height or crown diameter [7].

This paper is intended to summarize those recent developments. In addition, some new results concerning the imaging of full forest volumes are presented.

2 Single-Pass Millimeterwave SAR Tomography

In this section, a quick recap of millimeterwave SAR tomography with respect to forest areas is given. Since millimeterwave SAR systems certainly are much less common in remote sensing than X- or L-band systems, the characteristics of this particular microwave domain are first shortly sketched.

2.1 Advantages of Millimeterwave SAR

Typical wavelengths of millimeterwave frequencies differ from the common radar bands (L, C, X) in about one order of magnitude. For forest remote sensing, this leads to one significant advantage: It enables to achieve very high resolutions with comparably short synthetic apertures. Eventually, that means that images of vegetated areas can be well focused, because the blurring effect caused by wind-induced movements of leaves and branches etc. is reduced. This already provides a significant benefit when it comes to a detailed analysis of forested areas aiming at the single tree level.

In general, rough surfaces cause diffuse scattering, whereas smooth surfaces result in specular reflections. At millimeterwave frequencies, most surfaces appear rough, and diffuse scattering dominates the images, leading to coherent averaging within the resolution cells. Since this is an effect similar to multilook processing, the inherent speckle effect appears less severe than in common radar bands. In addition, the high sensitivity with respect to surface roughness certainly provides a benefit when analysis techniques based on distributed scatterers rather than deterministic point scatterers are used.

A more detailed discussion of the general peculiarities of millimeterwave SAR can be found in [8], for example. From the perspective of interferometric or tomographic techniques, two more aspects should be considered: First, the data should always be acquired by a single-pass system, which ensures high-coherent measurements, whereas repeat-pass systems usually decorrelate quickly for vegetated areas. Second, question arises about the amount of available volume penetration: While L-band or P-band SAR is expected to penetrate most (vegetation) volumes down to the ground, X- or C-band is usually expected to exhibit phase centers somewhere within the volume. In the millimeterwave domain (Ka-band to W-band), in contrast, canopy penetration is expected to be much less likely. An answer to this question based on real data experiments is one aspect of this paper.

2.2 Experimental System Description

For the experiments described in this paper, the German experimental sensor MEMPHIS is used as an exemplary single-pass millimeterwave TomoSAR system. The sensor was developed by the Fraunhofer Institute for High Frequency Physics and Radar Technology FHR in 1998 [9]. Although it can operate both in Ka-band (35 GHz) and W-band (94 GHz) and offers a fully polarimetric configuration, only the HH data of the Ka-band system are considered. In its interferometric configuration, MEMPHIS provides four receiving antennas, thus being a multi-baseline sensor with an overall baseline span (or elevation aperture) of 27.5 cm, which leads to a Rayleigh resolution of $\rho_\eta \approx 42$ m in elevation direction. The relevant system parameters can be found in Table 1.

System parameters	
Carrier frequency	35 GHz
Wavelength	8.543 mm
Acquisition parameters	
Flight heading angle	200 °
Flying altitude	760 m
Off-nadir angle	56 °
Slant range	1350 m
Resolution	
Azimuth	5.2 cm
Range	16.7 cm

Table 1: Parameters of the MEMPHIS test data.

2.3 TomoSAR Inversion for Discrete and Continuous Reflectivity Profiles

While TomoSAR basically aims at the reconstruction of continuous reflectivity profiles, it has also been adapted to and frequently used for discrete scenarios as they occur, e.g. in urban remote sensing [10,11]. Depending on the goal of tomographic analysis and on the utilized wavelength, in principle both models can be of interest for forested areas (cf. Fig. 1). A classic method that can be used for both continuous and discrete SAR tomography is the super-resolving, parametric MUSIC estimator [12]. Therefore, all experimental results presented in the following section are created with MUSIC.

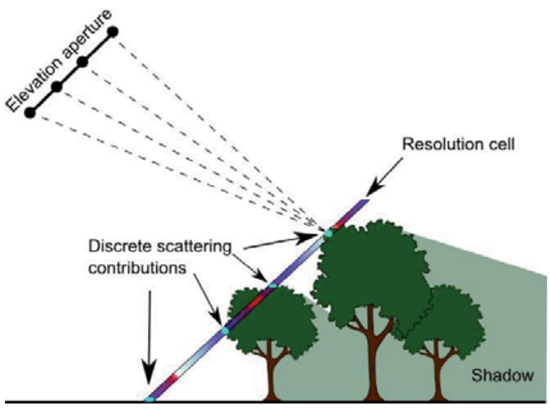

Figure 1: Sketch of the TomoSAR acquisition geometry for forested areas. If the continuous reflectivity hypothesis is used, the whole reflectivity profile of the resolution cell is reconstructed. If the discrete reflectivity hypothesis is used, only discrete scattering contributions at the sensor-facing tree structures are expected.

3 Experiments and Results

3.1 Test Data

For the experiments shown in this paper, data acquired by MEMPHIS during a flight campaign over Munich, Germany, in 2013 were used. The test scene contains the “Alter Nordfriedhof”, a former cemetery, which is used as a public park today. As can be seen in Fig. 2 (a), it's mainly characterized by a light planting of trees, resembling a grove or little wood. A corresponding SAR intensity image is shown in Fig. 2 (b). The model order map displayed in Fig. 2 (c) was calculated by the method described in [11]. Details about the test data are listed in Table 1.

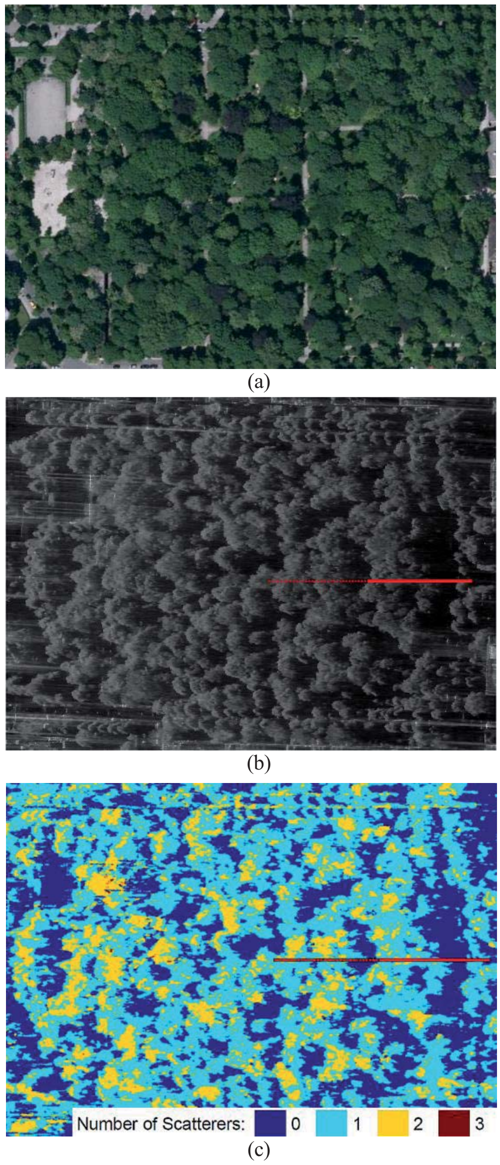

Figure 2: Test scene: (a) Optical image, (b) SAR intensity image (SAR range direction from left to right). (c) Model order map. The red marking indicates the test profile used in the experimental section: the solid line indicates the tomograms shown in Fig. 3, whereas the dashed line indicates the extension displayed in Fig. 4.

The ground truth used for comparison was acquired during a terrestrial laser scanning campaign in July 2014. From three scanning locations, three point clouds with approx. 35 million points each (point density approx. 2500 points/m^2) were created and co-registered afterwards. Details about the scanning system are summarized in Table 2.

System	Leica HDS700
Scanning type	Phase based
Wavelength	1.5 µm
Range	0.3 m … 187 m
Scan resolution	0.6 mm / 10 m
Angular resolution	7 µrad
Angular accuracy	125 µrad
Linearity error	≤ 1 mm

Table 2: Technical specifications of the terrestrial laserscanner used for ground truth generation.

3.2 Tomographic Slices

Figure 3 shows the tomographic slices corresponding to the solid line in Fig. 2, processed with MUSIC for a fixed model order of $K = 3$ (corresponding to the maximum degrees of freedom of a 4-antenna system such as MEMPHIS) as well as with automatic model order selection. Correspondingly, Fig. 3 (c) shows the discrete result corresponding to the peaks of the individual reflectivity profiles. Finally, the LiDAR ground truth projected into radar geometry is shown for comparison in Fig. 3 (d).

In order to provide more material for further analysis, additionally the MUSIC tomogram with automatic model order selection is provided in Fig. 4. It is extended by some range bins towards the sensor (marked by the dashed line in Fig. 2), discretized and geocoded as point cloud, with the points being colorized by the pseudo-intensities of the respective range-elevation cell. This way, the tomographic data can be overlayed with the LiDAR ground truth in world geometry.

From both the tomographic slices shown in Fig. 3 and the geocoded tomogram in Fig. 4, it can be seen that generally the main responses are located at the tree crowns facing the sensor. In addition, Fig. 3 (a) and the white box in Fig. 4 show that the tomographic data contains more information related to subcanopy scene content. Although actually covered by larger tree crowns, ground structures also exhibit a significant amount of backscatter. This indicates that millimeterwave SAR provides a certain amount of canopy penetration – at least if the canopy is not too dense.

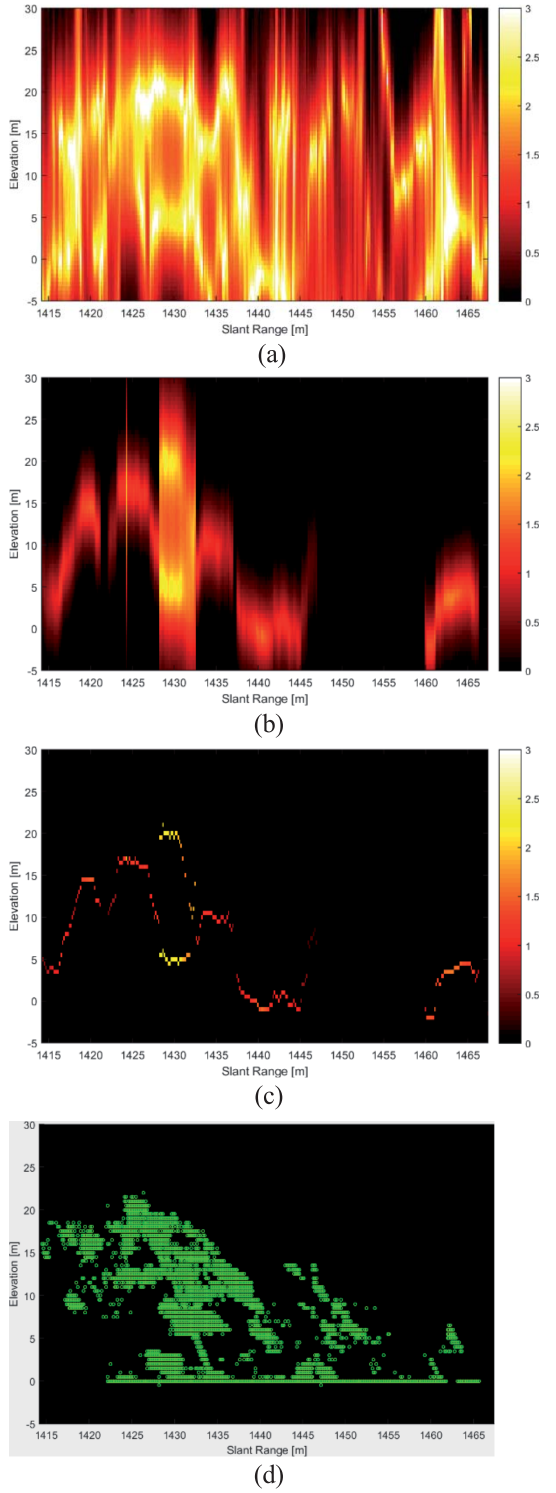

Figure 3: MUSIC tomograms (logarithmic pseudo-reflectivities) with (a) $K = 3$, (b) automatic model order selection. (c) Discretized tomogram corresponding to the peaks in (b). (d) LiDAR ground truth projected in radar geometry.

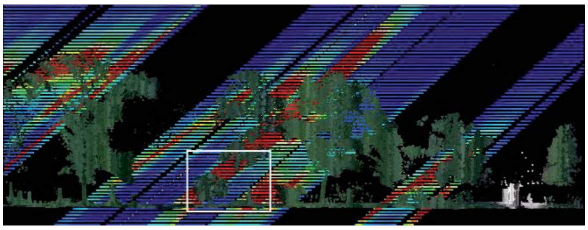

Figure 4: Geocoded MUSIC tomogram (automatic model order selection). The white box indicates the remarkable subcanopy response of a gravestone.

3.3 Individual Tree Reconstruction

Exploiting the fact that most backscattering occurs at the tree crowns, the sparse TomoSAR model can be used in order to create point clouds of the forested scene. Using a robust reconstruction approach focusing on the points belonging to the canopy, one can get rid of any points located at the ground or within tree crowns in order to reconstruct individual trees as model ellipsoids. The exemplary result for the test scene is shown in Fig. 5. More information on this topic can be found in [7].

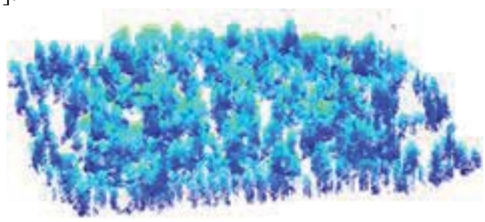

(a)

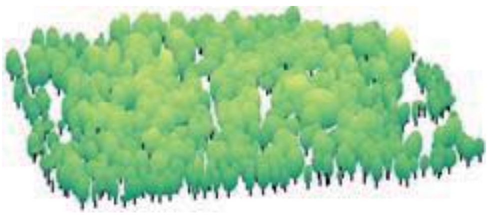

(b)

Figure 5: (a) Point cloud reconstructed using a discrete TomoSAR model. (b) Reconstructed tree models.

4 Summary and Conclusion

This paper presented experimental results concerning an analysis of forested areas by means of single-pass millimeterwave SAR tomography. Using test data acquired by the German multi-baseline interferometer MEMPHIS and a ground truth dataset acquired by high-precision terrestrial laser scanning, it could be shown that – although there is a certain amount of canopy penetration – a significant part of the response is received from the tree crowns. This enables both an analysis of forest volumes by continuous TomoSAR models as well as the reconstruction of canopy point clouds and individual tree models by utilization of discrete TomoSAR models.

Acknowledgment

The authors would like to thank T. Brehm and Dr. S. Stanko of Fraunhofer FHR for providing the MEMPHIS test data. In addition they want to thank C. Magnard and Dr. E. Meier of University of Zurich for focussing the raw SAR data. Finally, the efforts of TUM geodesists P. Schreiner and W. Wiedemann concerning the acquisition and processing of the LiDAR ground truth data are gratefully acknowledged.
This work is supported by the Helmholtz Association under the framework of the Young Investigators Group "SiPEO" (VH-NG-1018, www.sipeo.bgu.tum.de).

References

[1] A. Reigber, A. Moreira, "First demonstration of airborne SAR tomography using multibaseline L-band data," IEEE Trans. Geosci. Remote Sens., vol. 38, no. 5, pp. 2142–2152, 2000.

[2] O. Frey, F. Morsdorf, E. Meier, "Tomographic imaging of a forested area by airborne multi-baseline P-band SAR," Sensors, vol. 8, no. 9, pp. 5884–5896, 2007.

[3] O. Frey, E. Meier, "Analyzing tomographic SAR data of a forest with respect to frequency, polarization, and focusing technique," IEEE Trans. Geosci. Remote Sens., vol. 49, no. 10, pp. 3648–3659, 2011.

[4] S. Tebaldini, F. Rocca, "Multibaseline polarimetric SAR tomography of a boreal forest at P- and L-bands," IEEE Trans. Geosci. Remote Sens., vol. 50, no. 1, pp. 232–246, 2012.

[5] J. Praks, F. Kugler, J. Hyyppa, K. Papathanassiou, M. Hallikainen, "SAR coherence tomography for boreal forest with aid of laser measurements," in Proc. IGARSS, 2008, pp. 469–472.

[6] M. Schmitt, U. Stilla, "Generating point clouds of forested areas from airborne millimeter wave InSAR data," in Proc. IGARSS, 2014, pp. 1–4.

[7] M. Schmitt, M. Shahzad, X. Zhu, "Reconstruction of individual trees from multi-aspect TomoSAR data," Remote Sens. Environ., vol. 165, pp. 175–185, 2015.

[8] H. Essen, "Airborne remote sensing at millimeter wave frequencies," in Radar Remote Sensing of Urban Areas, U. Soergel, Ed. Dordrecht, Netherlands: Springer Science+Business Media, 2010.

[9] H. Schimpf, H. Essen, S. Boehmsdorff, T. Brehm, "MEMPHIS - a fully polarimetric experimental radar," in Proc. IGARSS, 2002, pp. 1714–1716.

[10] X. Zhu, R. Bamler, "Tomographic SAR inversion by L1-norm regularization - The compressive sensing approach," IEEE Trans. Geosci. Remote Sens., vol. 48, no. 10, pp. 3839–3846, 2010.

[11] M. Schmitt, U. Stilla, "Maximum-likelihood-based approach for single-pass synthetic aperture radar tomography over urban areas," IET Radar Sonar Nav., vol. 8, no. 9, pp. 1145–1153, 2014.

[12] R. O. Schmidt, "Multiple emitter location and signal parameter estimation," IEEE Trans. Antennas Propag., vol. 34, no. 3, pp. 276–280, 1986.